Survey of Machine Learning-based Predictions of Photovoltaic Power Outputs

Chbaro Mohamad and Salame Jean

Dar Al Handasah- Shair & Partner, Beirut, Lebanon

2023 Middle East and North Africa Solar Conference (MENA-SC) | 978-1-6654-9146-4/23/$31.00 ©2023 IEEE | DOI: 10.1109/MENA-SC54044.2023.10374517

***Abstract*—Solar Photovoltaic (PV) energy has been deployed at exponential rates since the last decade to produce power from renewable and green resources as a contribution to the causes of climate change and global warming. PV power generation is subject to very dynamic changes due to its dependence on the environment and the geography, often fluctuating erratically. The variability of PV power generation poses electric grid system stability, reliability, and planning downturns. Hence, grid operations could operate at higher levels of performance and efficiencies through adequate grid scheduling that primarily relies on accurate prediction of photovoltaic power output. Due to the paramount importance of the topic, the research community investigated several forecasting strategies that rely on numerical methods, probabilistic methods, physical models and machine learning-based (ML-based) techniques. The present paper presents a comparative review of the literature targeting ML-based algorithms for short-term PV power output prediction. A complementary case study exposes a much-needed homogeneous comparison of the state-of-the-art ML-based forecasters, trained on a dataset from the University of Liège. Model structural enhancement for the state-of-the-art is proposed and evaluated in the light of literature findings.**

I. INTRODUCTION

Global awareness on sustainable development caused an on-going exponential increase in the international integration of renewable energy technologies for power production. Photovoltaic power production received an important attention with the decrease of PV panel installation and operation and maintenance costs. Contributing hardware characteristics that incentivized PV integration include the increase in installation modularity, efficiency, service life and their contribution to lowering CO2 emissions and promoting environmental friendliness [1]. In the last few years, PV electric power generation has been integrated through large scale, residentially grid-connected and stand-alone systems [2]. Predictions claim that PV systems would drastically increase the sustainability of the global energy production spectrum with the contribution of PV-based power generation reaching up to 22% by 2050, allowing the globe to start benefitting from the desirable level of energy security [3, 4] [5].

PV power output is predominantly reliant on incident solar irradiations that reach the surface of the photovoltaic array (POA). A major variability in the PV power output is due to the deterministic fluctuations of POA irradiations caused by the diurnal cycle, characteristic of the Sun-Earth movement. Another significant factor is the stochastic behavior of the atmosphere which is controlled by the climatic-governance and the geographical-dependence of the PV plant. These weather variations are tracked at the scale of minutes, hours, days, weeks, years and decades. The associated weather variability is governed by meteorological factors including: cloud cover, visibility, air pressure, humidity levels, wind speed, temperature and many other [5] [6].

The mentioned geographical and meteorological variations lead to the intermittent nature of the power output, destabilizing grid operations and causing voltage surges, distortion in current and voltage waveforms, variations in frequency harmonic etc. To remediate and provide a reliable power management interface, frequency reserves and power storage facilities must be set in place [7] [8]. Hence, accurate PV power output forecasting would provide a crucial input to manage reserve capacities and schedule power consumption and production to provide functional grid operations and decrease PV integration costs. As a result, the research community is currently facing the challenge of making accurate forecasts of PV power generation [5] [6] [9] [10].

The present paper is contributing to the body of knowledge by presenting a review of the techniques used for intra-day and day-ahead PV output forecasting with a focus on machine learning algorithms to help guide future work in the field. A comparative case study is also conducted to present a homogeneous comparison of the top machine learning algorithms' forecast accuracy, quantifying the prediction error on a common test bed and proposing architecture improvements.

The major contributions of the present paper are summarized below:

1) Conduct on overview of short-term PV power output forecasters.
2) Determine the state-of-the-art models and conduct a comparative case study to evaluate their short-term performance on a common test bed using a 15min timestep.
3) Fine-tune the structure of the state-of-the-art models and highlights strengths and pitfalls.

The common test bed consists of a 48 days-long dataset holding meteorological measurements and PV output power

Authorized licensed use limited to: American University of Beirut. Downloaded on January 10,2024 at 12:32:15 UTC from IEEE Xplore. Restrictions apply.

measurements, collected at the Laboratory of Climatology at the University of Liège, located in Liège, Wallonia, Belgium [11]. The meteorological measurements include three cloud indexed (low, medium, high), precipitation, relative humidity, snow height, surface temperature, temperature 2m above ground level, wind speed at 10m from the ground, wind speed at 100m from the ground, global horizontal irradiance and top of atmosphere total solar irradiance. PV power output is recorded in 5 minutes-intervals.

II. Experiments & Results

This section gives an overview of the conducted experiments, results and formulates the analyses.
The 35-day dataset is split into 9:1 for training-testing with a chosen timestep is 15 minutes. LSTM and NARX-ANN models are executed on Jupyter Labs using Python environments and executed using Intel Core i7 CPU @ 2.2 GHz and 16GB of memory.

A. Dataset

The common test bed used in this paper to test, compare and evaluate the performance of the state-of-the-art models is a dataset available online, courtesy of the Laboratory of Climatology of the University of Liège, located in Liège, Wallonia, Belgium [11]. The PV plant in question has a nominal capacity of 466 kW. The dataset contains meteorological inputs from the 10th of May 2019 to the 18th of June 2019, recorded at 15-minutes intervals and PV power output inputs from the 13th of May 2019 to the 18th of June 2019, recorded at 15-seconds intervals.

The dataset contains the following meteorological measurements: three cloud indexed (low, medium, high), precipitation, relative humidity, snow height, surface temperature, temperature 2m above ground level, wind speed at 10m from the ground, wind speed at 100m from the ground, global horizontal irradiance and top of atmosphere total solar irradiance.

B. Data preprocessing

Meteorological and PV data display differences in terms of resolution and start dates which deemed data preprocessing necessary. PV data is resampled to the resolution of the weather data (15 minutes) using the average of the lower resolutions to dictate the resampled 15-min PV output. The meteorological data pertaining to the 10th through the 12th of May 2019 was deleted and the dataset is now combined into a single csv file attached to this paper. Meteorological input parameters and PV power output are shown in Figure 1 and measured PV plant power output in Figure 2. Dataset dates are parsed, and the min-max normalizer is applied to the whole dataset, which is then converted into a time-series.

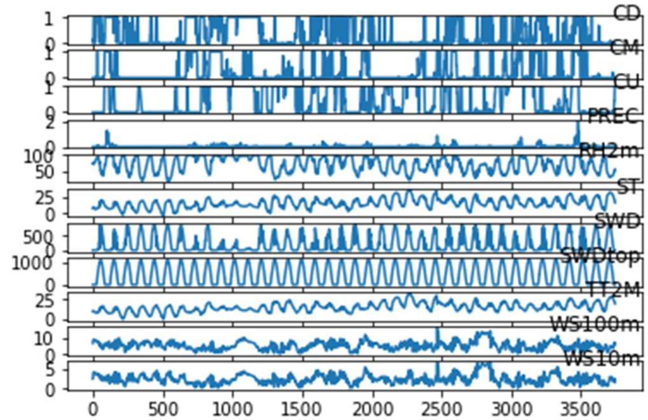

Fig. 1. Figure showing the weather input variations as a function of time before applying the min-max scaling method (time-series).

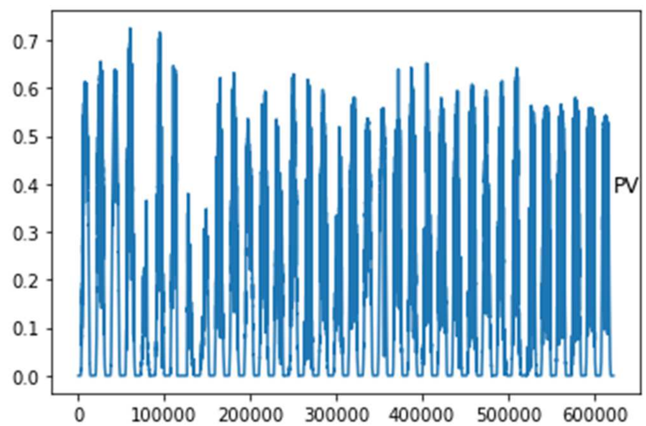

Fig. 2. Figure showing PV power output variations as a function of time before applying the min-max scaling method (time-series).

C. Experimental Setup: NARX-ANN Model

The NARX-ANN model is executed in a Python 2.7 environment using the PyNeurGen library [14]. The input layer contains 11 input nodes given that we have 11 input parameters, the hidden layer is composed of 3 neurons and the output layer is composed of a single neuron. The output and input order are respectively set to 1 and 2, which depicts the timestep used for predictions and inputs. The incoming weights from input and output are set to 0.5 and the model is initialized with random weights at all connections. The halt is set on extremes to act accordingly when experiencing extremely positive or negative numbers and the random constraints are set to 0.5. The learning rate is set to 0.1, the sigmoid function is used as an activation function for the layers. The model is trained with 15 epochs with disabled random testing.

D. Results and Analysis: NARX-ANN Model

The NARX-ANN model present in the literature successfully converged on the dataset with a mean squared error loss of 0.0087 and an optimal number of epochs of 3 epochs as shown in Figure 3. The predicted PV output is plotted against the real PV output in Figure 4. NARX-ANN is able to predict PV power values that fall within the range of the measured PV plant power output and it recognizes nighttime as zero power production.

Authorized licensed use limited to: American University of Beirut. Downloaded on January 10,2024 at 12:32:15 UTC from IEEE Xplore. Restrictions apply.

The pattern recognition ability of the model is reproducing increases and decreases of PV output that are identical to the measured ones, regardless of the change differential. Nonetheless, the pattern is recurring at a lag that is equal to the timestep (15 minutes), this could be due to the states that do not go through the non-linear propagation of ANN at every time step. This leaves the updated gradients, that are used to reconstruct the neural network, unchanged by the derivative of the non-linearity (magnitude less than 1). This characteristic of the algorithm preserve PV power fluctuation patterns and presents them at a lag equal to the timestep. It is important to note that the performance metric cited in the paper do not form a solid basis for comparison of model performance on the current dataset and the one used in the literature [12].

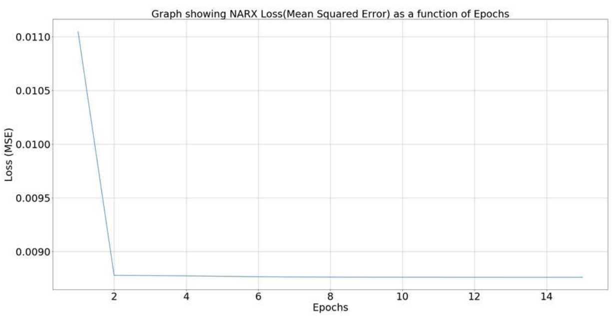

Fig. 3. Figure showing NARX model mean squared error (loss) as a function of training epochs.

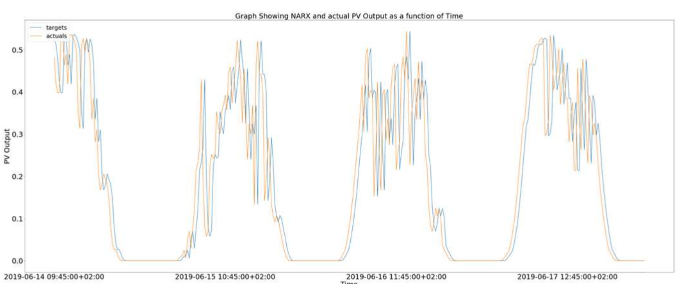

Fig. 4. Figure showing NARX PV forecasts and actual PV power measures as a function of time.

E. *Experimental Setup: LSTM Model*

The LSTM model is run in a Python 3 environment using the Keras library [15]. The first hidden layer of the LSTM model is allowed to return sequences to access the hidden state output for each input time step. It is constituted of 75 memory cells, a rectified linear activation function, a sigmoid activation function for the recurrent step. The second layer of the LSTM model is not allowed to returned sequences and is constituted of 70 memory cells. The default hyperbolic tangent activation function is used along with the sigmoid activation function for the recurrent step. The output layer consists of a dense layer with a single node. The model is combined using the mean squared error as a loss function, the Adam optimizer using accuracy as a metrics. The model is trained with 60 epochs and a batch size of 300 with disabled data shuffling.

F. *Results and Analysis: LSTM Model*

The state-of-the-art LSTM Model displayed a validation MSE loss (0.038) that is higher than the training loss (0.032) which depicts that the proposed model is not converging on the present test bed as shown in Figure 5. Hyperparameter tuning was conducted in section g and h to ensure model convergence. Nonetheless, the accuracy metric provided in the Keras library for training and testing (0.332; 0.303) is stable throughout epochs as shown in Figure 6. The predicted PV output is plotted against the real PV output in Figure 7. The LSTM predicts slightly negative values for PV output since it is unable to recognize night-time as zero power production, however, its pattern recognition ability is capturing the daytime sharp increases and decreases in power output. This ability comes from the structure of the memory cells that contain input, output and forget gates, which preserve daytime PV power fluctuation patterns. Moreover, LSTM forecasts are overall lower than the measured field data on the present test bed and in the state-of-the-art model [13]. When comparing the relevant metrics, this model performs better on the test bed when compared to the literature dataset with MAPEs of 8.8% versus 22.3% [13]..

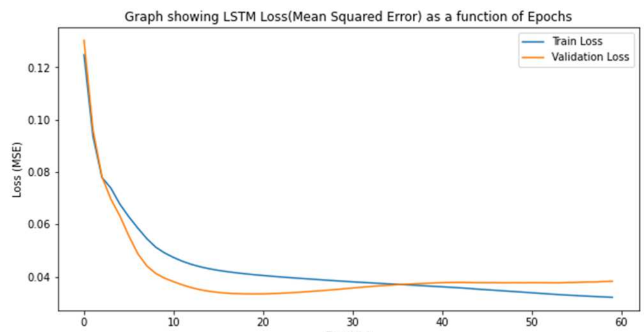

Fig. 5. Figure showing LSTM model mean squared error losses for training and validation data as a function of training epochs.

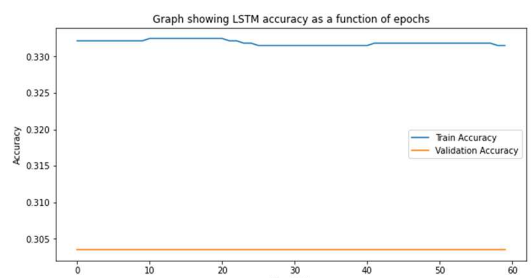

Fig. 6. Figure showing LSTM model training and validation accuracies as a function of training epochs.

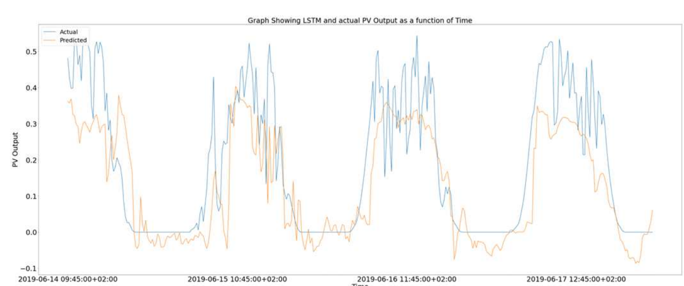

Fig. 7. Figure showing LSTM PV forecasts and actual PV power measures as a function of time.

Authorized licensed use limited to: American University of Beirut. Downloaded on January 10,2024 at 12:32:15 UTC from IEEE Xplore. Restrictions apply.

G. *Experimental Setup: Proposed Enhanced LSTM Model*

The proposed enhanced LSTM model has the same number of input parameters, hidden layers, memory cells, activation functions, hidden state return sequences, and output dense layer as described in *Section E*. The loss function, optimizer and accuracy metrics are left unchanged from *Section E*'s description. Regularization is implemented as a strategy to ensure model convergence and improve accuracy metrics. Regularization was implemented on the first hidden layer (75 memory cells) of the state-of-the-art LSTM model described in *Section E*. The dropout rate applied to the hidden layer aims at tuning an overfitting model and improve model performance by probabilistically excluding activation and weight updates of a certain percentage of recurrent connections. A dropout rate of 40% is applied to the first LSTM hidden layer (as shown in Figure 8) and the model is trained with 100 epochs and a batch size of 300 with disabled data shuffling.

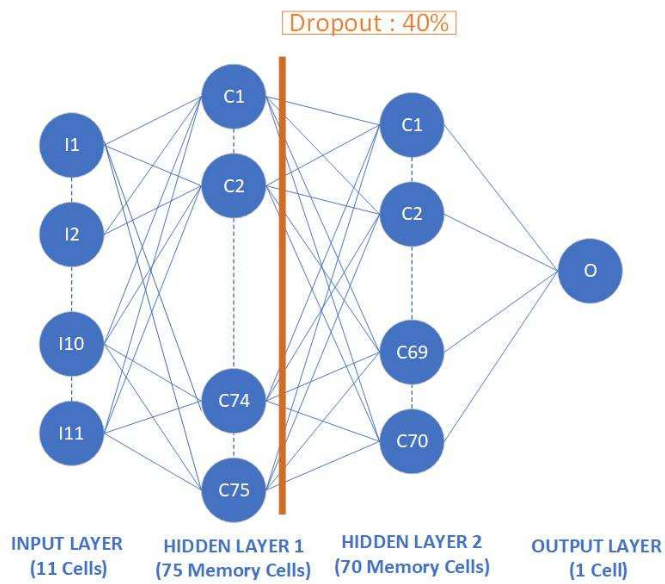

Fig. 8. Figure showing the structure and architecture of the proposed enhanced LSTM model with the 40% dropout rate on the first hidden layer.

H. *Results and Analysis: Proposed Enhanced LSTM Model*

The proposed enhanced LSTM Model displayed validation and training MSE losses of 0.035 which depicts a converging model as shown in Figure 9. The dropout rate of 40% removed the overfitting tendency, however it provided similar Keras accuracy metrics for training and testing (0.332; 0.303) is stable throughout epochs as shown in Figure 10. The predicted PV output of state-of-the-art and enhanced LSTM forecasters are plotted against the real PV output in Figure 11. This proposed model tends to capture higher extreme values and to predict higher PV power output during daytime and more negative values during nighttime. Comparable to the state-of-the-art method, it is also unable to recognize nighttime as zero power output, however, its pattern recognition ability is more exaggerated than the state-of-the-art LSTM model. This ability comes from the same reasons stated in *Section E*.

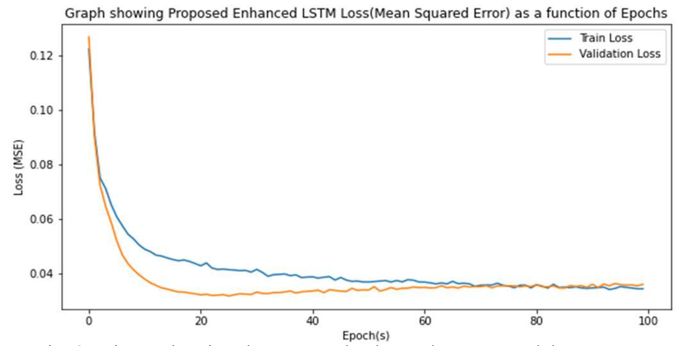

Fig. 9. Figure showing the proposed enhanced LSTM model mean squared error losses for training and validation data as a function of training epochs.

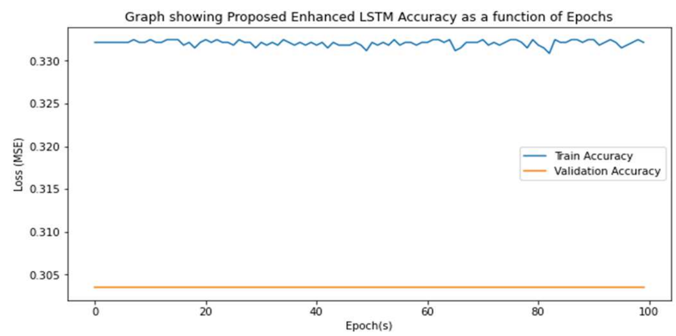

Fig. 10. Figure showing proposed enhanced LSTM model training and validation accuracies as a function of training epochs.

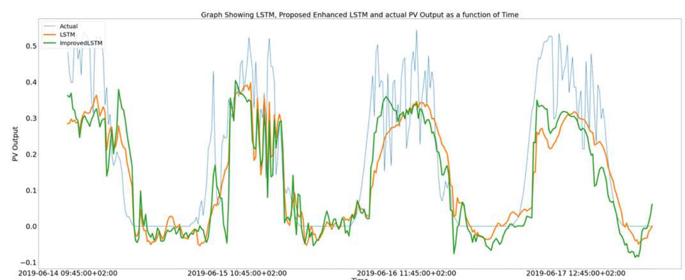

Fig. 11. Figure showing state-of-the-art LSTM and proposed enhanced PV forecasts and actual PV power measures as a function of time.

TABLE V
HYBRID-BASED TABLE SHOWING PERFORMANCE METRICS FOR LITERATURE AND TESTED/PROPOSED PV OUTPUT

	NARX		LSTM		
	Literature	STOA	Literature	STOA	Improved
RMSE	0.0002	0.183	0.71	0.119	0.114
MAE	N/A	18.3%	N/A	8.8%	7.9%
MAPE	1.74%	0.2	22.3%	8.8%	7.9%

Comparing the performance metrics of Table V, literature and experimental accuracy cannot be compared for NARX because MSE is specific to the magnitude of the data and cannot be generalized as a standalone value. Comparing the MARX model to the LSTM model, all performance metrics affirm that LSTM predictions outperform NARX predictions. Comparing the model described in the literature to the proposed LSTM model with an enhanced architecture and structure, its prediction performance metrics are better than the literature-based LSTM, which is diverging and overfitting the data. Figure 12 displays the three forecasting models in question and

Authorized licensed use limited to: American University of Beirut. Downloaded on January 10,2024 at 12:32:15 UTC from IEEE Xplore. Restrictions apply.

the actual plant measured PV power output as a function of time.

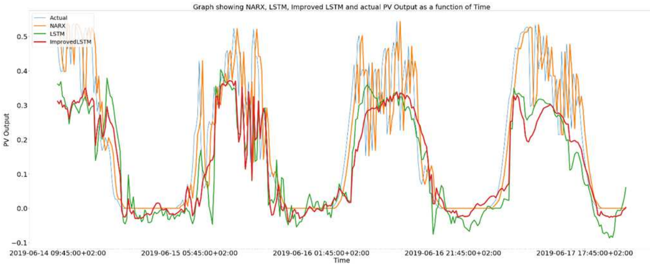

Fig. 12. Figure showing NARX, state-of-the-art LSTM, proposed enhanced PV forecasts and actual

III. Conclusion

This paper presents a wide-spectrum of the Machine Learning, Deep Learning and Hybrid-based PV power output forecasting methods available in the literature. The examined state-of-the-art models are Long Short-Term Memory (LSTM) and Nonlinear Auto Regressive models with eXogenous input (NARX). This paper evaluated these models along with their architecture and structure, as reported in the literature, on a common testbed with a unified data train/test ratio and a common timestep of 15 minutes. This paper determined that an enhanced version of the LSTM model reported in the literature is the most accurate for PV power output forecaster according to performance metrics. Nonetheless, the NARX-ANN model displayed slightly inferior metrics (as per Table XXX) but was able to accurately replicate PV fluctuation patterns with a lag that is equal to the timestep. This lag can be explained by the states that do not go through the non-linear propagation of ANN due to the low magnitude of the derivative of the updated gradients that reconstruct the network. The pattern recognition and replication abilities of LSTM are inferior to the ones presented by NARX. This is due to the structure of the memory cells that contain a multitude of gates. Thereby, NARX is best suited for applications that rely on the peak PV output.

Additional comparative studies would be the subject of future works in the field of PV output prediction and would target GA-optimized deep learning models. Moreover, evaluating the added value that the hybrid LSTM and NARX models provide on top of each one of the model alone would start by showing the added value of framework such as Evolution of Recurrent Systems with Optimal Linear Output (EVOLINO) [16].

References

[1] Raza MQ, Nadarajah M, Ekanayake C. On recent advances in PV output power forecast. Sol Energy 2016;136:125–44.

[2] A. Reinders, P. Verlinden, A. Freundlich, Photovoltaic Solar Energy: from Fundamentals to Applications, John Wiley & Sons, 2017.

[3] IRENA, Global Energy Transformation, A Roadmap to 2050, Tech. rep., IRENA, Abu Dhabi, 2018. http://www.irena.org/publications/2018/Apr/Global- Energy-Transition-A-Roadmap-to-2050..

[4] IEA, Technology Roadmap Solar Photovoltaic Energy, International Energy Agency (IEA).

[5] M.Q. Raza, M. Nadarajah, C. Ekanayake, On recent advances in PV output power forecast, Sol. Energy 136 (2016).

[6] J. Antonanzas, N. Osorio, R. Escobar, R. Urraca, F. Martinez-de Pison, F. Antonanzas-Torres, Review of photovoltaic power forecasting, Sol. Energy 136 (2016) 78-111.

[7] T. AlSkaif, W. Schram, G. Litjens, W. van Sark, Smart charging of community storage units using Markov chains, in: IEEE PES Innovative Smart Grid Tech- nologies Conference Europe (ISGT-Europe), IEEE, 2017, pp. 1-6, 2017.

[8] T. Terlouw, T. AlSkaif, C. Bauer, W. van Sark, Multi-objective optimization of energy arbitrage in community energy storage systems using different battery technologies, Appl. Energy 239 (2019) 356-372.

[9] Mellit, A. Massi Pavan, V. Lughi, “Deep learning neural networks for short-term photovoltaic power forecasting.” Renewable Energy. Volume 172, 2021, Pages 276-288 ISSN 0960-1481

[10] B. Elsinga, W.G. van Sark, Short-term peer-to-peer solar forecasting in a network of photovoltaic systems, Appl. Energy 206 (2017) 1464e1483..

[11] "Liege Microgrid Open Data," Laboratory of Climatology of the University of Liège, 2019. [Online]. Available: https://www.kaggle.com/jonathandumas/liege-microgrid-open-data?select=miris_pv.csv. [Accessed 01 November 2020].

[12] I. Sansa et al, "PV power forecasting using different artificial neural networks strategies," in 2014, . DOI: 10.1109/ICGE.2014.6835397.

[13] M. S. Hossain and H. Mahmood, "Short-Term Photovoltaic Power Forecasting Using an LSTM Neural Network and Synthetic Weather Forecast," IEEE Access, vol. 8, pp. 172524-172533, 2020..

[14] Smiley D. PyNeurGen: Python Neural Genetic Algorithm Hybrids. Release 0.3, URL http://pyneurgen.sourceforge.net 2012. [Online].

[15] "Keras: Deep Learning library for Theano and TensorFlow,," [Online]. Available: https://keras.io/.

[16] M. Massaoudi et al, "A Novel Approach Based Deep RNN Using Hybrid NARX-LSTM Model For Solar Power Forecasting" 2019.

Authorized licensed use limited to: American University of Beirut. Downloaded on January 10,2024 at 12:32:15 UTC from IEEE Xplore. Restrictions apply.